Reconstruction of Multidimensional Bandlimited Signals From Nonuniform and Generalized Samples

Arie Feuer, *Fellow, IEEE*, and Graham C. Goodwin, *Fellow, IEEE*

***Abstract*—This paper addresses the problem of multidimensional signal reconstruction from nonuniform or generalized samples. Typical solutions in the literature for this problem utilize continuous filtering. The key result of the current paper is a multidimensional "interpolation" identity, which establishes the equivalence of two multidimensional processing operations. One of these uses continuous domain filters, whereas the other uses discrete processing. This result has obvious benefits in the context of the afore mentioned problem. The results here expand and generalize earlier work by other authors on the one-dimensional (1-D) case. Potential applications include two-dimensional (2-D) images and video signals.**

***Index Terms*—Multidimensional sampling, nonuniform sampling, reconstruction.**

I. Introduction

DISCRETE multidimensional signal processing inherently relies on sampling a continuous multivariable signal. In this way, a multidimensional discrete representation of the signal is obtained. By a multidimensional signal, we mean a signal that depends on more than one variable [examples include two-dimensional (2-D) images and three-dimensional (3-D) video]. The most common form of sampling is on a lattice which is the multidimensional equivalent of uniform sampling in the one-dimensional (1-D) case. (A brief overview of lattices will be provided in the next section.) In many applications, however, the data inherently has a more complex structure. For example, it might be generated by nonuniform sampling or by sampling multichannel versions of the original signals.

Two specific applications which have motivated the author's interest in the questions addressed in the current paper are i) resolution enhancement of fiberoptic endoscopes and ii) resolution enhancement and video compression in digital video cameras. In the first of these applications, the fiberoptic size and the endoscope diameter put a constraint on possible image resolution as each fiber transfers a single pixel of the image. In this project, we generate multiple images with temporal changes and use them to generate a single image of improved resolution. In the second application, one uses multiple video cameras to capture different aspects of the same scene. Some may emphasize spatial resolution whilst others may emphasize temporal resolution, i.e., frame rate. The problem is then to use the multiple clips to gain a single video clip with enhanced resolution: both spatial and temporal. The problem is made more difficult because each camera will have a different sampling pattern. Some details of these applications are commercially sensitive at this stage, but the basic technical issues involved are addressed in the two specific patterns analyzed in Sections IV and V of this paper.

Reconstruction of signals from *uniform* sampling (i.e. on a lattice) is a straightforward generalization of the one-dimensional (1-D) case using lowpass filters (see, e.g., [2], [9], and [14]). However, existing methods for reconstruction from other types of data, such as those mentioned above, typically use continuous filters (see, e.g., [1] and [3]) and are thus unsuitable for digital implementation.

In [4], the authors address the above issues for the 1-D case. Specifically, they introduce a result coined the "Interpolation Identity." This identity is shown to lead to efficient reconstruction methods from generalized samples, as well as efficient interpolation to uniformly spaced samples.

In the current paper, we generalize the results presented in [4] to multidimensional signals. Potential applications of the results described here would include the following:

- taking digital photographs of the same scene using identical or different digital cameras;
- analyzing video images of the same scene taken by different cameras.

The resultant identity is, in fact, a statement of equivalence between two configurations to process sampled data signals having a continuous signal as output. In one of the configurations, the processing is done in the continuous domain using continuous filters. In the alternative configuration, the processing is done in the discrete domain. A key property of the second configuration is that it leads to a discrete representation having "uniform" samples (i.e. sampled on a lattice). If required, the continuous signal can be recovered form these "uniform samples" via a multivariable lowpass filtering operation [2]. However, in other cases, the conversion to uniform samples (on a lattice) could be a desirable end-point in its own right.

The layout of the remainder of the paper is as follows. In Section II, we provide a brief overview of multidimensional sampling and introduce the notation to be used in the sequel. In Section III, we state and prove the key result of this paper, namely, a multidimensional version of the "Interpolation identity" introduced in [4] for the 1-D case. This involves several novel aspects that are not present in the 1-D case. Section IV and Section V consider two cases of multidimensional recurrent

Manuscript received September 13, 2004; revised January 25, 2005. The associate editor coordinating the review of this manuscript and approving it for publication was Dr. Ta-Hsin Li.

A. Feuer is with the Department of Electrical Engineering, Technion–Israel Institute of Technology, Haifa 32000, Israel (e-mail: feuer@ee.technion.ac.il).

G. C. Goodwin is with School of Electrical Engineering and Computer Science, University of Newcastle, Callaghan, Australia.

Digital Object Identifier 10.1109/TSP.2005.857047

sampling based on the Generalized Sampling Expansion (GSE) (see, e.g., [1] and [6]). For these cases, the multidimensional Interpolation Identity is applied to generate an efficient implementation algorithm.

II. Background to Multidimensional Sampling

A. Sampling Lattices and Noncommutative Rings

The generalization of the concept of uniform sampling in the 1-D case to multivariable sampling leads to the notion of a "sampling lattice" (see, e.g., [2]). By a sampling *lattice*, we refer to a set

$$\mathcal{LAT}(T) = \{T\underline{n} : \underline{n} \in \mathbb{Z}^D\} \subset \mathbb{R}^D \tag{1}$$

for a given nonsingular matrix $T \in \mathbb{R}^{D\times D}$. Here, we have used $\mathbb{Z}$, $\mathbb{R}$ to denote the integers and reals, respectively. The generalization of a "sampling interval" in the 1-D case to the multidimensional case leads to the concept of a *unit cell*. A unit cell $\mathcal{UC}(T) \subset \mathbb{R}^D$ associated with the sampling lattice $\mathcal{LAT}(T)$ is a set with the following two properties: $\{\mathcal{UC}(T) + T\underline{n}_1\} \cap \{\mathcal{UC}(T) + T\underline{n}_2\} = \varnothing$ for any $\underline{n}_1, \underline{n}_2 \in \mathbb{Z}^D$, $\underline{n}_1 \neq \underline{n}_2$, and $\bigcup_{\underline{n}\in\mathbb{Z}^D} \{\mathcal{UC}(T) + \underline{n}\} = \mathbb{R}^D$. A given lattice gives rise to many unit cells. However, all possible unit cells of the same lattice have an identical volume given by $|\det(T)|$. A *set of representatives* of a given lattice over the integers $\mathcal{LAT}(K)$, where K is an integer matrix, is defined to be the set

$$\mathcal{SR}(K) = \mathcal{UC}(K) \cap \mathcal{LAT}(I) \tag{2}$$

where I is the identity matrix (hence, $\mathcal{LAT}(I) = \mathbb{Z}^D$). Clearly, since the unit cell is not unique, neither is $\mathcal{SR}(K)$. However, it can be shown (see [8]) that the number of elements in every $\mathcal{SR}(K)$ is the same and is equal to $|\det(K)|$.

Important insights into sampling lattices are also provided from their equivalent frequency domain representations. In this context, one can either use normalized frequencies (as is often done in the signal processing literature) or unnormalized frequencies (as discussed in detail in [7]). Both are equivalent, and thus, it is a matter of taste as to which one decides to use for a given problem. In this paper, we will use unnormalized frequencies since by doing so, we maintain the same scale of the frequency domain operator, which allows easier comparison of the effect of different sampling patterns.

Using these ideas, then for every sampling lattice $\mathcal{LAT}(T)$, there exists a *polar* (or *reciprocal*) lattice defined by $\mathcal{LAT}(2\pi T^{-T})$ with the property that $\underline{\omega}^T\underline{x}$ is an integer multiple of 2π for every $\underline{\omega} \in \mathcal{LAT}(2\pi T^{-T})$, $\underline{x} \in \mathcal{LAT}(T)$. The reciprocal lattice plays a key role for signals sampled on $\mathcal{LAT}(T)$. In particular, it represents the frequency domain effect of sampling on $\mathcal{LAT}(T)$. This is analogous to the relationship between $\{n\Delta t\}$ and $\{k(2\pi/\Delta t)\}$ in the 1-D case.

The above points highlight the core difference between the 1-D and multidimensional cases. Specifically, in the 1-D case, we need to deal with integers (i.e., a *commutative ring*), whereas in the multidimensional case, we will need to deal with square matrices of integers (i.e., a *noncommutative ring*). This key difference leads to major difficulties in the multidimensional case, both in terms of the formulation and derivation of results. One aspect of this difficulty is highlighted in [15], where it is pointed out that the lack of commutativity prevents decimators and expanders to be commuted in the multidimensional case (see also [10] or [5]). This particular issue was later resolved in [8]. This reference also introduces various tools of which we will make use of and generalize in the sequel.

For completeness, we summarize below some facts regarding noncommutative rings we will utilize. See [11], [12], [15], and, in particular, [8] for further details.

Given three matrices $M, M_o, S \in \mathbb{Z}^{D\times D}$, which satisfy $M = SM_o$, we call S a *left devisor* of M. M is called a *left multiple* of M_o. A *greatest common left (right) divisor* (g.c.l.d. or g.c.r.d) $S \in \mathbb{Z}^{D\times D}$ of two matrices M, $R \in \mathbb{Z}^{D\times D}$ is a common left (right) divisor that is a right (left) multiple of every common left (right) devisor of M and R. $S \in \mathbb{Z}^{D\times D}$ is said to be unimodular if $|\det(S)| = 1$. M and R are *left (right) coprime* if their g.c.l.d (g.c.r.d) is unimodular. It is known that (see, e.g., [8]) for every left coprime nonsingular M_o and R_o, there exists right coprime pairs $\widetilde{M}_o$, $\widetilde{R}_o \in \mathbb{Z}^{D\times D}$ such that $M_o^{-1}R_o = \widetilde{R}_o\widetilde{M}_o^{-1}$ with $|\det(M_o)| = |\det(\widetilde{M}_o)|$. Hence, one can readily observe that for any nonsingular integral M, R, there exist a pair $\widetilde{M}$, $\widetilde{R}$ for which

$$\begin{aligned} M^{-1}R &= \widetilde{R}\widetilde{M}^{-1} \\ |\det(M)| &= \left|\det(\widetilde{M})\right|. \end{aligned} \tag{3}$$

We illustrate the last point by the following simple example (this example will be utilized in the sequel to further illustrate multidimensional sampling ideas and concepts).

Example 1: Let

$$M = \begin{bmatrix} 2 & 1 \\ 0 & 2 \end{bmatrix};\ R = \begin{bmatrix} 1 & 0 \\ 1 & 3 \end{bmatrix}. \tag{4}$$

Then, we can choose

$$\widetilde{M} = \begin{bmatrix} 4 & -3 \\ 0 & -1 \end{bmatrix};\ \widetilde{R} = \begin{bmatrix} 1 & 0 \\ 2 & -3 \end{bmatrix} \tag{5}$$

and properties (3) can readily be verified. ■

B. Preliminary Results

We assume that the continuous signals, which we denote $f_c(\underline{x})$, $\underline{x} \in \mathbb{R}^D$, are bandlimited in the sense that there exists a sampling lattice $\mathcal{LAT}(T_Q)$ with the property that

$$\text{support}\left(\widehat{f}_c(\underline{\omega})\right) \subseteq \mathcal{UC}\left(2\pi T_Q^{-T}\right) \tag{6}$$

Here, and elsewhere, we use $\hat{\gamma}(\underline{\omega})$ to denote the multidimensional Fourier transform of the signal $\gamma(\underline{x})$.

The lattice $\mathcal{LAT}(T_Q)$ can be viewed as the multivariable generalization of the "Nyquist rate" in the 1-D case. For this reason, we call it a "Nyquist lattice."

Clearly, the signal $f_c(\underline{x})$ could be reconstructed from its sampled values on $\mathcal{LAT}(T_Q)$ by passing $f_d(\underline{x}) = \sum_{\underline{n}\in\mathbb{Z}^D} f_c(T_Q\underline{n})\delta(\underline{x} - T_Q\underline{n})$ through the ideal lowpass filter

$$\widehat{h}_{LP}(\underline{\omega}) = \begin{cases} |\det(T_Q)|, & \text{for } \underline{\omega} \in \mathcal{UC}\left(2\pi T_Q^{-T}\right) \\ 0, & \text{otherwise} \end{cases} \tag{7}$$

However, our interest here is in generalized sampling. Thus, we assume that the actual sampling lattice we employ is $\mathcal{LAT}(T)$.

We impose the following constraint on the relationship between $\mathcal{LAT}(T)$ and $\mathcal{LAT}(T_Q)$:

Assumption 1: T and T_Q are related via

$$\begin{aligned} T &= T_Q M^{-1} R \\ &= T_Q \widetilde{R} \widetilde{M}^{-1} \end{aligned} \tag{8}$$

where R, M, $\widetilde{R}$, and $\widetilde{M} \in \mathbb{Z}^{D\times D}$ are nonsingular matrices satisfying (3). ■

Note that Assumption 1 is not very restrictive. Indeed, in the scalar case, it simply reduces to the fact that the ratio T/T_Q is rational. In the multivariable case, a sufficient condition is that the entries in T and T_Q are rational.

Assumption 1 (8) guarantees that $\mathcal{LAT}(T_Q)$ (the Nyquist lattice) can be generated from $\mathcal{LAT}(T)$ through expansion of $\mathcal{LAT}(T)$ by a factor of R and then decimation by a factor of M. These operations, for the multidimensional case, are discussed and demonstrated in Section II-C (see also [15]).

Let M, $\widetilde{M} \in \mathbb{Z}^{D\times D}$ be as in (3). We next consider the lattices $\mathcal{LAT}(M^T)$, $\mathcal{LAT}(\widetilde{M}^T)$, together with any of their respective unit cells $\mathcal{UC}(M^T)$, $\mathcal{UC}(\widetilde{M}^T)$ and their sets of representatives $\mathcal{SR}(M^T)$ and $\mathcal{SR}(\widetilde{M}^T)$. Clearly, since $|\det(M^T)| = |\det(\widetilde{M}^T)|$, the two sets of representatives contain the same number of distinct vectors N. These observations are illustrated below.

Example 1 (Continued): The above concepts are illustrated in Fig. 1 for the example matrices given in (4) and (5). For the unit cells in Fig. 1, we have $N = |\det(M^T)| = 4$. In particular, $\mathcal{SR}(M^T) = \{\left[\begin{smallmatrix}0\\0\end{smallmatrix}\right], \left[\begin{smallmatrix}0\\1\end{smallmatrix}\right], \left[\begin{smallmatrix}1\\1\end{smallmatrix}\right], \left[\begin{smallmatrix}1\\2\end{smallmatrix}\right]\}$ and $\mathcal{SR}(\widetilde{M}^T) = \{\left[\begin{smallmatrix}0\\0\end{smallmatrix}\right], \left[\begin{smallmatrix}1\\-1\end{smallmatrix}\right], \left[\begin{smallmatrix}2\\-2\end{smallmatrix}\right], \left[\begin{smallmatrix}3\\-3\end{smallmatrix}\right]\}$.

Note that by definition, for every $\underline{m} \in \mathbb{Z}^D$, there exist unique $\underline{n}, \widetilde{\underline{n}} \in \mathbb{Z}^D$, and $\underline{k} \in \mathcal{SR}(M^T)$, $\widetilde{\underline{k}} \in \mathcal{SR}(\widetilde{M}^T)$ such that $\underline{m} = M^T\underline{n} + \underline{k} = \widetilde{M}^T\widetilde{\underline{n}} + \widetilde{\underline{k}}$ (see [15]). We can then write $\underline{m} \equiv \underline{k} \bmod (M^T)$ and $\underline{m} \equiv \widetilde{\underline{k}} \bmod (\widetilde{M}^T)$. We thus have the following result, which gives an explicit enumeration of $\mathcal{SR}(M^T)$ and $\mathcal{SR}(\widetilde{M}^T)$.

Lemma 1: The mapping $\rho : \mathcal{SR}(M^T) \to \mathcal{SR}(\widetilde{M}^T)$ defined by

$$\begin{aligned} \rho(\underline{k}) &\equiv (\widetilde{R}^T \underline{k}) \bmod (\widetilde{M}^T) \\ &= \widetilde{R}^T \underline{k} - \widetilde{M}^T \underline{n} \end{aligned} \tag{9}$$

is one to one and onto.

Proof: (See Appendix A). ■

We illustrate by continuing the example.

Example 1 (continued): For the matrices in the example, we apply ρ as introduced in Lemma 1 and obtain

$$\rho\left\{\begin{bmatrix}0\\0\end{bmatrix}, \begin{bmatrix}0\\1\end{bmatrix}, \begin{bmatrix}1\\1\end{bmatrix}, \begin{bmatrix}1\\2\end{bmatrix}\right\} = \left\{\begin{bmatrix}0\\0\end{bmatrix}, \begin{bmatrix}2\\-2\end{bmatrix} \begin{bmatrix}3\\-3\end{bmatrix}, \begin{bmatrix}1\\-1\end{bmatrix}, \right\}. \quad ■$$

An immediate consequence of Lemma 1 is that we can enumerate the vectors $\underline{k}_1, \ldots, \underline{k}_N$ in $\mathcal{SR}(M^T)$ and $\widetilde{\underline{k}}_1, \ldots, \widetilde{\underline{k}}_N$ in $\mathcal{SR}(\widetilde{M}^T)$ such that

$$\widetilde{\underline{k}}_\ell = \rho(\underline{k}_\ell), \text{ for } \ell = 1, 2, \ldots, N. \tag{10}$$

In the analysis presented below, in order to simplify notation, we describe discrete signals as weighted sums of Dirac Delta functions. This enables us to view them as continuous signals and eliminates the need to distinguish between continuous and discrete (normalized) frequencies. Hence, *we only use continuous frequencies* $\underline{\omega} \in \mathbb{R}^D$. The same holds for the filters we use, i.e., a discrete filter will have an impulse response, which is a weighted sum of Dirac Delta functions and a frequency response that is *periodic* over the corresponding reciprocal lattice.

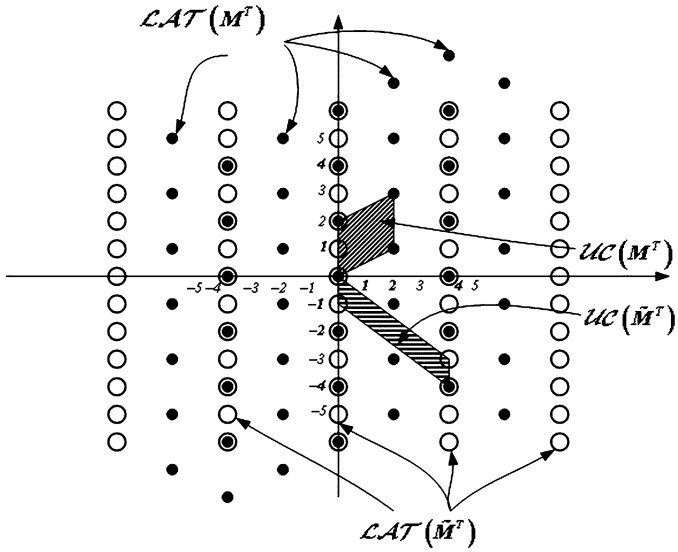

Fig. 1. Lattices $\mathcal{LAT}(M^T)$ and $\mathcal{LAT}(\widetilde{M}^T)$ and their respective unit cells for the example.

C. Multivariable Upsampling and Downsampling

In our development presented later, we will utilize expanding by a matrix factor R (multivariable upsampling) and decimating by a matrix factor M (multivariable downsampling)—both R and M are matrices of integers. In essence, these operations are similar to those used in the scalar case; however, the technical details can be significantly more intricate. Say, the initial sampling lattice is $\mathcal{LAT}(T)$. When expanded by R, we get the lattice $\mathcal{LAT}(TR^{-1}) \supseteq \mathcal{LAT}(T)$, and when decimated by M, we get the lattice $\mathcal{LAT}(TR^{-1}M) = \mathcal{LAT}(T_Q) \subseteq \mathcal{LAT}(TR^{-1})$. As a demonstration, see Fig. 2, where we chose

$$T = \begin{bmatrix} \frac{1}{4} & -\frac{3}{4} \\ \frac{1}{2} & \frac{3}{2} \end{bmatrix}.$$

We also choose T_Q as the 2×2 identity matrix and R, M as in the example; one can readily verify that Assumption 1 holds for these choices. The initial lattice $\mathcal{LAT}(T)$ is presented in Fig. 2 by solid circles, the empty circles are $\mathcal{LAT}(TR^{-1})$, and "$\times$" denotes $\mathcal{LAT}(TR^{-1}M)$. We see from the figure the relationships $\mathcal{LAT}(T) \subseteq \mathcal{LAT}(TR^{-1})$ and $\mathcal{LAT}(TR^{-1}M) \subseteq \mathcal{LAT}(TR^{-1})$. For a more detailed exposition on this subject, see [15].

III. Key Technical Result

In this section, we state and prove our key result, which is a multivariable interpolation identity. This establishes an equivalence between a continuous multivariable filterbank and a discrete filtering scheme involving upsampling and downsampling. The result extends a published result [4] for the 1-D case to the multidimensional case. The two configurations are illustrated in Figs. 3 and 4, respectively. These figures have been introduced

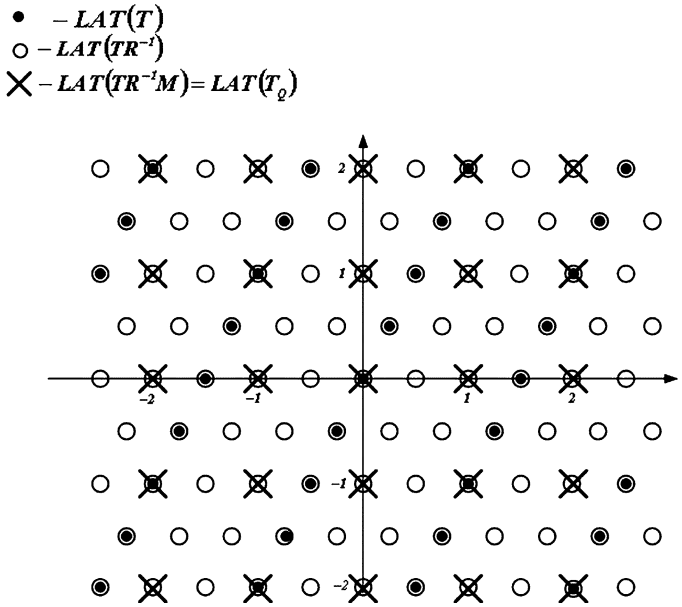

Fig. 2. Input lattice $\mathcal{LAT}(T)$, expanded by R, to give $\mathcal{LAT}(TR^{-1})$ and decimated by M to give $\mathcal{LAT}(TR^{-1}M)$.

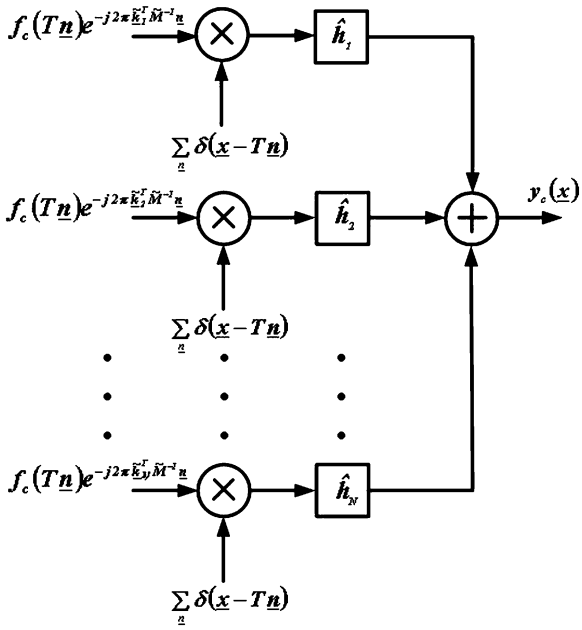

Fig. 3. Continuous filterbank configuration.

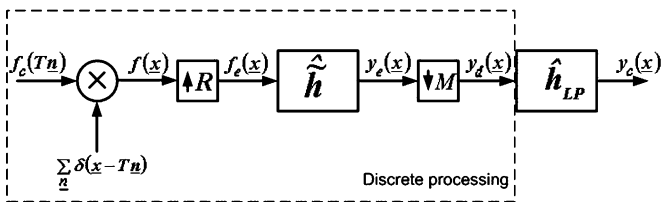

Fig. 4. Equivalent discrete configuration.

so that we can better visualize the result. Both configurations are driven by the multivariable sampled data of $f_c(\underline{x})$, $\underline{x}\in\mathbb{R}^D$ sampled on $\mathcal{LAT}(T)$. However, the processing in Fig. 3 is all in the continuous domain, whereas in Fig. 4, most of the processing is done in the discrete domain. Only in the last step in Fig. 4, a standard lowpass filter [as given in (7)], which allows reconstruction from data sampled on a lattice, is continuous. The setup described in Fig. 3 is motivated by the most general reconstruction problem we treat, namely, the Pth-order nonuniform sampling. We present this problem and illustrate the utility of our result in Section V.

We further wish to point out that the filters $\{h_\ell(\underline{x})\}_{\ell=1}^N$ in Fig. 3 are bandlimited to $\mathcal{UC}(2\pi T_Q^{-T})$ (which is also the bandwidth of the signal $f_c(\underline{x})$). The signals $f(\underline{x})$, $f_e(\underline{x})$, $y_e(\underline{x})$, and $y_d(\underline{x})$ in Fig. 4 are all discrete signals (i.e., sequences). The same is true for the filter $\widetilde{h}(\underline{x})$, which is denoted by its frequency response $\widehat{\widetilde{h}}(\underline{\omega})$ in Fig. 4. Note that $\widehat{\widetilde{h}}(\underline{\omega})$ is periodic, since it represents discrete processing (hence, its impulse response is a weighted sum of Dirac Delta functions). In addition, note that the signal $f_e(\underline{x})$ is the result of expanding $f(\underline{x})$ by a factor R, and $y_d(\underline{x})$ results from decimating $y_e(\underline{x})$ by a factor M, where both R and M are (integral) matrices.

Given the above background, we are now in a position to state and prove the following.

Theorem 1: Let $f_c(\underline{x})$ be such that (6) is satisfied. Consider T, T_Q, satisfying Assumption 1, with M, R, $\widetilde{M}$, $\widetilde{R}$ as in (8) and $\{\underline{k}_\ell\}_{\ell=1}^N=\mathcal{SR}(M^T)\{\underline{\widetilde{k}}_\ell\}_{\ell=1}^N=\mathcal{SR}(\widetilde{M}^T)$ enumerated so that (10) holds. Then, the configurations in Figs. 3 and 4 are equivalent, provided we choose

$$\widehat{\widetilde{h}}(\underline{\omega})=\frac{N}{|\det(T_Q)|}\sum_{\underline{n}\in\mathbb{Z}^D}\sum_{\ell=1}^{N}\widehat{h}_\ell\left(\underline{\omega}-2\pi T_Q^{-T}\underline{k}_\ell+2\pi T_Q^{-T}M^T\underline{n}\right). \tag{11}$$

Proof: See Appendix B. ■

Remark 1: For the scalar case, Assumption 1 becomes $T/T_Q=R/M$ for any coprime integers M, R. This generalizes the result in [4], where it is assumed that $T/T_Q-1/M$ is an integer [namely, $R\equiv 1 \bmod (M)$].

Remark 2: Note that by virtue of (11), the resultant filter $\widehat{\widetilde{h}}(\omega)$ is indeed periodic in the expanded reciprocal lattice $\mathcal{LAT}(2\pi T^{-T}R^T)=\mathcal{LAT}(2\pi T_Q^{-T}M^T)$, i.e., $\widehat{\widetilde{h}}(\underline{\omega}+2\pi T_Q^{-T}M^T\underline{n})=\widehat{\widetilde{h}}(\underline{\omega})$ for all $\underline{\omega}$. Furthermore, (11) can be thought of as a tiling process over one "period" in the frequency domain, i.e., over a unit cell of $\mathcal{LAT}(2\pi T^{-T}R^T)$. This unit cell is divided into $N=|\det(M)|$ unit cells of the reciprocal "Nyquist" lattice $\mathcal{LAT}(2\pi T_Q^{-T})$. In each of the unit cells, we place the shifted frequency response of one continuous filter. This process is illustrated in Fig. 5 for the simple example above. In this figure, we demonstrate how the unit cell $\mathcal{UC}(2\pi T^{-T}R^T)$ of the lattice $\mathcal{LAT}(2\pi T^{-T}R^T)$ (which is the period of filter $\widehat{\widetilde{h}}(\omega)$) is constructed from the unit cell of the "Nyquist lattice" $\mathcal{LAT}(2\pi T_Q^{-T})$ shifted by $2\pi T_Q^{-T}\underline{k}_\ell$ and how each period of $\widehat{\widetilde{h}}(\omega)$ is constructed from the filters $\widehat{h}_\ell(\omega)$ shifted by $2\pi T_Q^{-T}\underline{k}_\ell$, respectively.

As an illustration of the utility of the above result, we apply it, in the following sections, to some special cases, namely, the reconstruction of a signal sampled on recurrent sampling patterns.

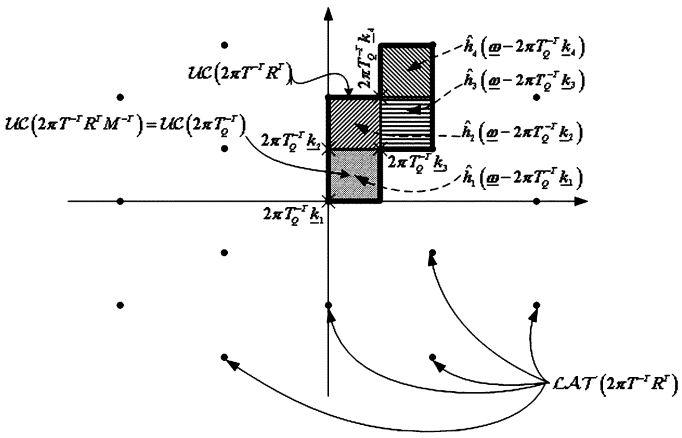

Fig. 5. Demonstration of the "tiling" construction of $\hat{\hat{h}}(\underline{\omega})$, as defined in (11).

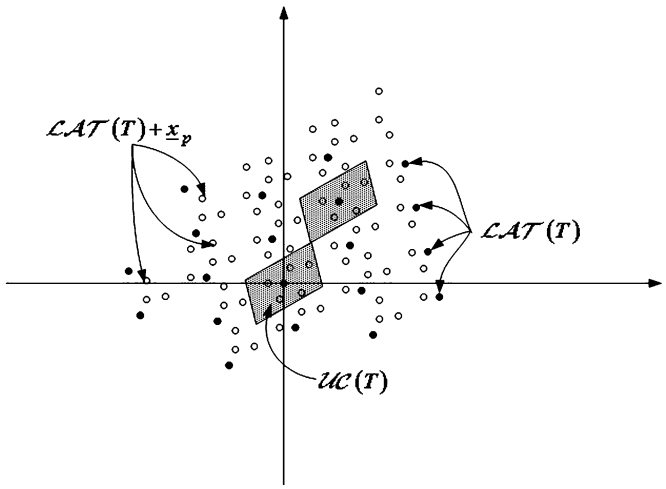

Fig. 6. Two-dimensional example of recurrent sampling.

IV. Multidimensional Recurrent Nonuniform Sampling

In this section, we consider a special case of multidimensional nonuniform sampling. Let $\mathcal{LAT}(T_Q)$ and $\mathcal{LAT}(T)$ be two sampling lattices. Assume that

$$T = T_Q R \tag{12}$$

for some nonsingular $R \in \mathbb{Z}^{D\times D}$. Thus, clearly, $\mathcal{LAT}(T) \subset \mathcal{LAT}(T_Q)$. The sampling pattern we consider here is defined by

$$\Psi = \bigcup_{p=1}^{P} \left\{\mathcal{LAT}(T) + \underline{x}_p\right\} \quad \underline{x}_p \in \mathbb{R}^D. \tag{13}$$

This sampling pattern is commonly referred to as a *recurrent sampling pattern*; see, e.g., [2]. A 2-D example is presented in Fig. 6. The solid circles, in Fig. 6, represent the points of $\mathcal{LAT}(T)$ and the hollow circles the additional points. Note that the pattern of the added samples in each shifted unit cell of $\mathcal{LAT}(T)$ is identical. The union of these sets is a recurrent sampling pattern Ψ. A specific example of this situation arises when one utilizes multiple identical digital cameras on the same scene.

In the 1-D case (see, e.g., [4]), the *number* of distinct points added in each sampling period (unit cell) of $\mathcal{LAT}(T)$ determines the bandwidth of reconstructible signals. The corresponding multidimensional case is more complex, as we show below. Let $\underline{c}_l = 2\pi T^{-T}\underline{k}_l \in \mathcal{LAT}(2\pi T^{-T})$, where $\{\underline{k}_l\}_{l=1}^{L} = \mathcal{SR}(R^T)$, and $L = |\det(R)|$. Then, it can be shown that

$$\mathcal{UC}\left(2\pi T_Q^{-T}\right) = \bigcup_{l=1}^{L} \left\{\mathcal{UC}(2\pi T^{-T}) + \underline{c}_l\right\}. \tag{14}$$

Note that a similar construction has been demonstrated in Fig. 5 (see Remark 2).

Consider next a bandlimited signal $f_c(\underline{x})$ such that

$$\text{support}\left(\widehat{f}_c(\underline{\omega})\right) \subseteq \mathcal{UC}\left(2\pi T_Q^{-T}\right) = \bigcup_{l=1}^{L} \left\{\mathcal{UC}(2\pi T^{-T}) + \underline{c}_l\right\}. \tag{15}$$

Thus, $\mathcal{LAT}(T_Q)$ is a "Nyquist lattice" for this signal.

In the sequel, we make extensive use of the Generalized Sampling Expansions (GSEs) results (see [1], [6], and [13]). For the benefit of the reader, we formally restate the most general form of this result below:

Theorem 2: Let $f_c(\underline{x}), T_Q$, and T be as in (12) and (15). Suppose $f_c(\underline{x})$ is passed through a bank of L filters $\{\widehat{h}_p(\underline{\omega})\}_{p=1}^{L}$ to generate the signals $g_p(\underline{x})$. Namely, $\widehat{g}_p(\underline{\omega}) = \widehat{h}_p(\underline{\omega})\widehat{f}_c(\underline{\omega})$. Then, a necessary and sufficient condition that $f_c(\underline{x})$ can be reconstructed from $\{g_p(T\underline{n})\}_{p=1}^{L}$ is that the equation

$$\begin{bmatrix} \widehat{h}_1(\underline{\omega}+\underline{c}_1) & \cdots & \widehat{h}_P(\underline{\omega}+\underline{c}_1) \\ \vdots & \ddots & \vdots \\ \widehat{h}_1(\underline{\omega}+\underline{c}_L) & \cdots & \widehat{h}_P(\underline{\omega}+\underline{c}_L) \end{bmatrix} \begin{bmatrix} \Phi_1(\underline{\omega},\underline{x}) \\ \Phi_2(\underline{\omega},\underline{x}) \\ \vdots \\ \Phi_P(\underline{\omega},\underline{x}) \end{bmatrix} = \begin{bmatrix} e^{j\underline{c}_1^T\underline{x}} \\ e^{j\underline{c}_2^T\underline{x}} \\ \vdots \\ e^{j\underline{c}_L^T\underline{x}} \end{bmatrix} \tag{16}$$

has a solution for all $\underline{x}$ and every $\underline{\omega} \in \mathcal{UC}(2\pi T^{-T})$. Under these conditions, the reconstruction is given by

$$f_c(\underline{x}) = \sum_{p=1}^{P} \sum_{\underline{n}\in\mathbb{Z}^D} g_p(T\underline{n})\varphi_p(\underline{x} - T\underline{n}) \tag{17}$$

where

$$\varphi_p(\underline{x}) = \frac{|\det(T)|}{(2\pi)^D} \int_{\mathcal{UC}(2\pi T^{-T})} \Phi_p(\underline{\omega},\underline{x}) e^{j\underline{\omega}^T\underline{x}} d\underline{\omega} \tag{18}$$

and Φ_p are a solution of (16).

Proof: See [6]. ■

We now return to recurrent sampling such that $f_c(\underline{x})$ is sampled on Ψ [see (13)]. This problem can be reformulated as a special case of the GSE described in Theorem 2. Choosing $\widehat{h}_p(\underline{\omega}) = e^{j\underline{\omega}^T\underline{x}_p}$, we get $g_p(\underline{x}) = f_c(\underline{x} + \underline{x}_p)$, and sampling each on $\mathcal{LAT}(T)$ results in the same data as by the recurrent sampling. We can now readily apply Theorem 2. Specifically, we have for the case of interest here that

$$\begin{bmatrix} \widehat{h}_1(\underline{\omega}+\underline{c}_1) & \cdots & \widehat{h}_P(\underline{\omega}+\underline{c}_1) \\ \vdots & \ddots & \vdots \\ \widehat{h}_1(\underline{\omega}+\underline{c}_L) & \cdots & \widehat{h}_P(\underline{\omega}+\underline{c}_L) \end{bmatrix} = H \cdot \text{diag}\left\{e^{j\underline{\omega}^T\underline{x}_p}\right\} \in \mathbb{C}^{L\times P} \tag{19}$$

where

$$H = \begin{bmatrix} e^{j\underline{c}_1^T \underline{x}_1} & e^{j\underline{c}_1^T \underline{x}_2} & \cdots & e^{j\underline{c}_1^T \underline{x}_P} \\ e^{j\underline{c}_2^T \underline{x}_1} & e^{j\underline{c}_2^T \underline{x}_2} & \cdots & e^{j\underline{c}_2^T \underline{x}_P} \\ \vdots & \vdots & \ddots & \vdots \\ e^{j\underline{c}_L^T \underline{x}_1} & e^{j\underline{c}_L^T \underline{x}_2} & \cdots & e^{j\underline{c}_L^T \underline{x}_P} \end{bmatrix} \tag{20}$$

and (16) has a solution if H has *full row rank* (see [6]). A necessary condition for this to hold is, clearly, that $L \leq P$. We assume, in the sequel, that $L = P$ and that the matrix H is nonsingular. Then, the reconstruction is carried out using (17) and (18).

Equation (17) can also be rewritten in an equivalent convolution form

$$f_c(\underline{x}) = \sum_{p=1}^{L} f_p(\underline{x}) * \varphi_p(\underline{x}) \tag{21}$$

where

$$f_p(\underline{x}) = \sum_{\underline{n} \in \mathbb{Z}^D} f_c(T\underline{n} + \underline{x}_p)\delta(\underline{x} - T\underline{n}). \tag{22}$$

This form of the result is depicted in Fig. 7. We further illuminate this result below.

Let us denote $G = H^{-1}$; then, from (16) and (19), we have

$$\Phi_p(\underline{\omega}, \underline{x}) = e^{-j\underline{\omega}^T \underline{x}_p} \sum_{l=1}^{L} G_{p,l} e^{j\underline{c}_l^T \underline{x}}$$

and

$$\varphi_p(\underline{x}) = \frac{|\det(T)|}{(2\pi)^D} \int_{\mathcal{UC}(2\pi T^{-T})} e^{j\underline{\omega}^T(\underline{x} - \underline{x}_p)} d\underline{\omega} \sum_{l=1}^{L} G_{p,l} e^{j\underline{c}_l^T \underline{x}}. \tag{23}$$

Then

$$\begin{aligned} \widehat{\varphi}_p(\underline{\omega}) &= \int_{\mathbb{R}^D} \varphi_p(\underline{x}) e^{-j\underline{\omega}^T \underline{x}} d\underline{x} \\ &= \frac{|\det(T)|}{(2\pi)^D} \sum_{l=1}^{L} G_{p,l} \int_{\mathcal{UC}(2\pi T^{-T})} \left[\int_{\mathbb{R}^D} e^{-j(\underline{\omega} - \underline{c}_l - \underline{\eta})^T \underline{x}} d\underline{x} \right] \\ &\quad \times e^{-j\underline{\eta}^T \underline{x}_p} d\underline{\eta} \\ &= |\det(T)| \sum_{l=1}^{L} G_{p,l} \int_{\mathcal{UC}(2\pi T^{-T})} \delta(\underline{\omega} - \underline{c}_l - \underline{\eta}) e^{-j\underline{\eta}^T \underline{x}_p} d\underline{\eta} \\ &= \sum_{l=1}^{L} G_{p,l} e^{-j(\underline{\omega} - \underline{c}_l)^T \underline{x}_p} \widehat{h}_{LP}(\underline{\omega} - \underline{c}_l; \mathcal{UC}(2\pi T^{-T})) \end{aligned} \tag{24}$$

where we have used notation similar to the one in [4] for the ideal lowpass filter

$$\widehat{h}_{LP}\left(\underline{\omega}; \mathcal{UC}(2\pi T^{-T})\right) = \begin{cases} |\det(T)|, & \text{for } \underline{\omega} \in \mathcal{UC}(2\pi T^{-T}) \\ 0, & \text{otherwise} \end{cases} \tag{25}$$

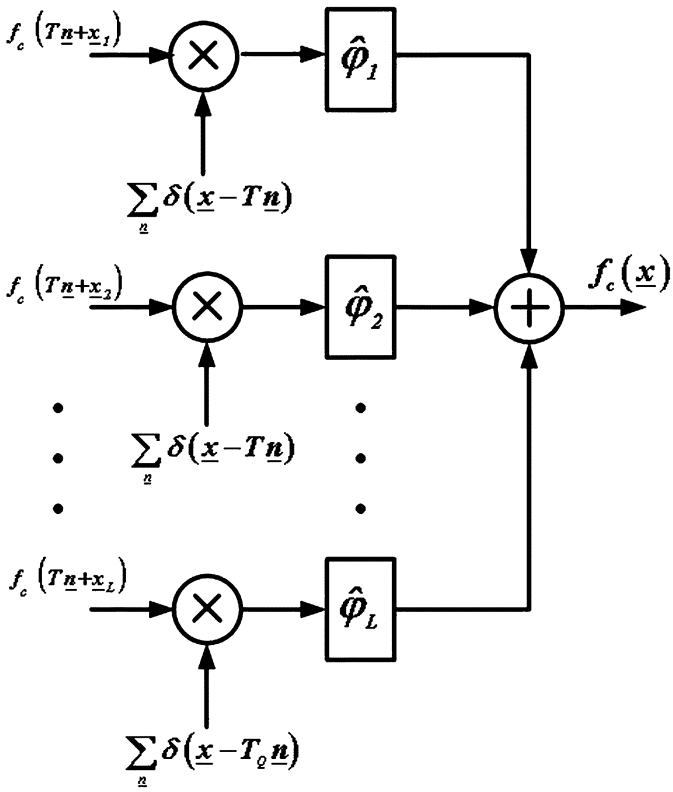

Fig. 7. Reconstruction from recurrent nonuniform sampling.

We see from (14), (16), (18), and (19) that $\widehat{\varphi}_p(\underline{\omega}) = 0$ for all $\underline{\omega} \notin \mathcal{UC}(2\pi T_Q^{-T})$, namely, the filters $\widehat{\varphi}_p(\underline{\omega})$ are bandlimited to the same bandwidth as the signal $f_c(\underline{x})$. Thus, the reconstruction in Fig. 7 is achieved via continuous filtering.

We will next utilize Theorem 1 to show how discrete filtering can be employed for this problem. To this end, we directly apply the result of Theorem 1 to each branch of Fig. 7. This is illustrated in Fig. 8, where, in this case, the discrete filters satisfy

$$\begin{aligned} \widehat{\widehat{h}}_p(\underline{\omega}) &= \sum_{\underline{n} \in \mathbb{Z}^D} \widehat{\varphi}_p\left(\underline{\omega} + 2\pi T_Q^{-T} \underline{n}\right) \\ &= \frac{1}{|\det(T_Q)|} \sum_{l=1}^{L} G_{p,l} e^{-j\left(\underline{\omega} - \underline{c}_l + 2\pi T_Q^{-T} \underline{n}\right)^T \underline{x}_p} \\ &\quad \times \widehat{h}_{LP}\left(\underline{\omega} - \underline{c}_l + 2\pi T_Q^{-T} \underline{n}; \mathcal{P}(\Lambda^*)\right). \end{aligned} \tag{26}$$

Thus, using Theorem 1, we have generated the samples on a Nyquist lattice. In many applications, this will be the desired end result. However, if the continuous signal is required, then one need only apply the low pass filter $\widehat{h}_{LP}(\omega; \mathcal{UC}(2\pi T_Q^{-T}))$ as shown on the far right hand side of Fig. 8.

V. Multidimensional Pth-Order Nonuniform Sampling

In Section IV, the sampling used consisted of shifted versions of the *same* lattice. A further embellishment arises when one uses *distinct* lattices. A specific application would be the use of multiple cameras, each having a distinctive sampling pattern.

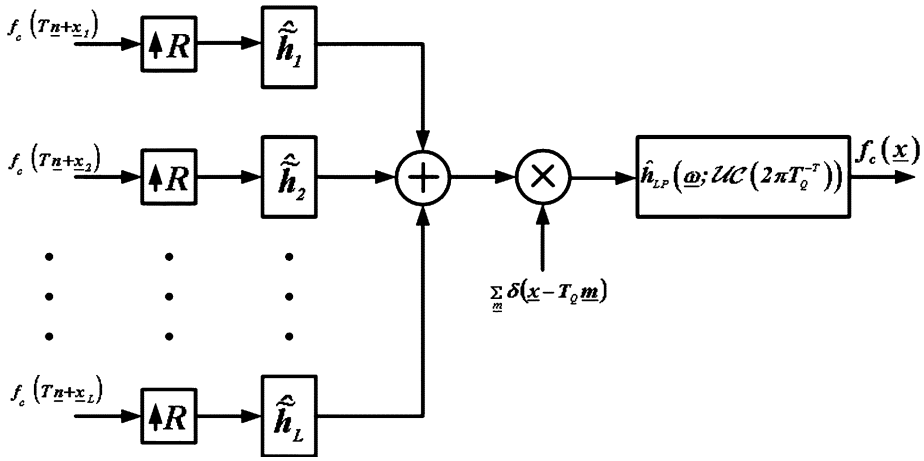

Fig. 8. Discrete filterbank reconstruction from recurrent nonuniform sampling.

The combined sampling pattern in this case can be described as

$$\Psi = \bigcup_{p=1}^{P} \{\mathcal{LAT}(T_p) + \underline{x}_p\} \quad \underline{x}_p \in \mathbb{R}^D. \tag{27}$$

We again assume that there exist a "Nyquist" sampling lattice $\mathcal{LAT}(T_Q)$ and consider signals satisfying

$$\text{support}\left(\widehat{f}(\underline{\omega})\right) \subseteq \mathcal{UC}\left(2\pi T_Q^{-T}\right). \tag{28}$$

We also assume that for each T_p, we have

$$\begin{aligned} T_p &= T_Q \widetilde{R} \widetilde{M}_p^{-1} \\ &= T_Q M_p^{-1} R_p \end{aligned} \tag{29}$$

with $|\det(M_p)| = |\det(\widetilde{M}_p)|$ for some nonsingular integral matrices $\widetilde{R}$, M_p. Note that there is no loss of generality in assuming that $\widetilde{R}$ is common to all T_p since if it is not, we can always choose $\widetilde{R} = l.c.r.m(\widetilde{R}_p) = \widetilde{R}_p \widetilde{S}_p$ and replace the $\widetilde{M}_p$ by $\widetilde{M}_p \widetilde{S}_p$, maintaining the ratio and resulting in the form of (29).

We wish to reconstruct the signal $f(\underline{x})$ from its samples on Ψ, namely, from the data set $\{f(\underline{x}) : \underline{x} \in \Psi\}$. Denoting

$$T = T_Q \widetilde{R} \tag{30}$$

we obtain from (29)

$$T_p = T \widetilde{M}_p^{-1}. \tag{31}$$

Furthermore, let

$$\{\underline{\widetilde{m}}_{p,r}\}_{r=1}^{L_p} = \mathcal{SR}(\widetilde{M}_p) \tag{32}$$

where $L_p = |\det(\widetilde{M}_p)|$.

It can then be readily shown that

$$\Psi = \bigcup_{p=1}^{P} \bigcup_{r=1}^{L_p} \{\mathcal{LAT}(T) + \underline{x}_p + T_p \underline{\widetilde{m}}_{p,r}\}. \tag{33}$$

Once put in this form, we can see that this problem is a special case of the recurrent sampling discussed in the previous section. Hence, denoting $L = |\det(\widetilde{R})|$, we need to have $L \leq \sum_{p=1}^{P} L_p$. We will assume $L = \sum_{p=1}^{P} L_p$, and, as in (15), that

$$\mathcal{UC}\left(2\pi T_Q^{-T}\right) = \bigcup_{q=1}^{P} \bigcup_{l=1}^{L_p} \{\mathcal{UC}(2\pi T^{-T}) + \underline{c}_{q,l}\} \tag{34}$$

where $\underline{c}_{q,l} = 2\pi T^{-T} \underline{\widetilde{n}}_{q,l}$ and $\bigcup_{q=1}^{P} \{\underline{\widetilde{n}}_{q,l}\}_{l=1}^{L_p} = \mathcal{SR}(\widetilde{R}^T)$. (The two indexed enumeration is adopted for notational convenience.)

Using (20) and (33), the resulting matrix H will have the form

$$H = \begin{bmatrix} H^{1,1} & \cdots & H^{1,P} \\ \vdots & \ddots & \vdots \\ H^{P,1} & \cdots & H^{P,P} \end{bmatrix} \tag{35}$$

where the (q,p)th block is (36), shown at the bottom of the page. Assuming H is invertible with $G = H^{-1}$, the reconstruction formula, using continuous filtering, can then be obtained as in (17)–(24), i.e.,

$$f(\underline{x}) = \sum_{p=1}^{P} \sum_{r=1}^{L_p} \sum_{\underline{n} \in \mathbb{Z}^D} f(T\underline{n} + \underline{x}_p + T_p \underline{\widetilde{m}}_{p,r}) \varphi_{p,r}(\underline{x} - T\underline{n}) \tag{37}$$

$$H^{q,p} = \begin{bmatrix} e^{j\underline{c}_{q,1}^T(\underline{x}_p + T_p \underline{\widetilde{m}}_{p,1})} & e^{j\underline{c}_{q,1}^T(\underline{x}_p + T_p \underline{\widetilde{m}}_{p,2})} & \cdots & e^{j\underline{c}_{q,1}^T\left(\underline{x}_p + T_p \underline{\widetilde{m}}_{p,L_p}\right)} \\ e^{j\underline{c}_{q,2}^T(\underline{x}_p + T_p \underline{\widetilde{m}}_{p,1})} & e^{j\underline{c}_{q,2}^T(\underline{x}_p + T_p \underline{\widetilde{m}}_{p,2})} & \cdots & e^{j\underline{c}_{q,2}^T\left(\underline{x}_p + T_p \underline{\widetilde{m}}_{p,L_p}\right)} \\ \vdots & \vdots & \ddots & \vdots \\ e^{j\underline{c}_{q,L_q}^T(\underline{x}_p + T_p \underline{\widetilde{m}}_{p,1})} & e^{j\underline{c}_{q,L_q}^T(\underline{x}_p + T_p \underline{\widetilde{m}}_{p,2})} & \cdots & e^{j\underline{c}_{q,L_q}^T\left(\underline{x}_p + T_p \underline{\widetilde{m}}_{p,L_p}\right)} \end{bmatrix} \in \mathbb{C}^{L_q \times L_p} \tag{36}$$

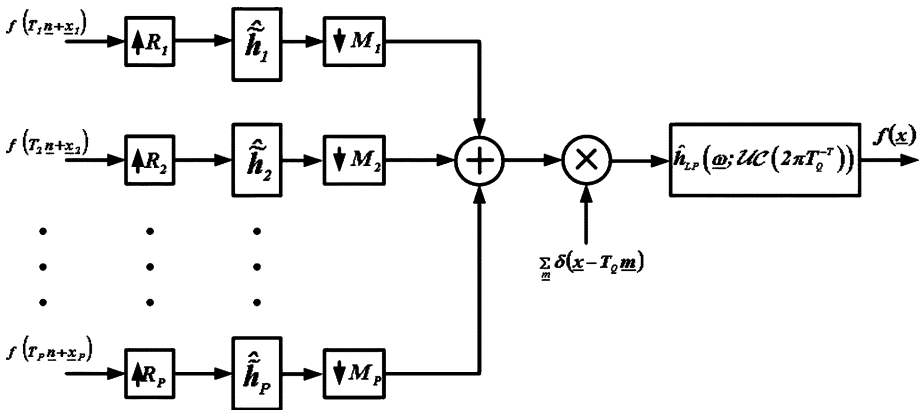

Fig. 9. Reconstruction from Pth nonuniform sampling using a discrete filterbank.

where

$$\varphi_{p,r}(\underline{x})=\frac{|\det(T)|}{(2\pi)^D}\int_{\mathcal{UC}(2\pi T^{-T})}e^{j\underline{\omega}^T(\underline{x}-\underline{x}_p-T_p\widetilde{\underline{m}}_{p,r})}d\underline{\omega}\times\sum_{q=1}^{P}\sum_{l=1}^{L_q}(G^{p,q})_{r,l}e^{j\underline{c}_{q,l}^T\underline{x}}. \quad (38)$$

The reconstruction formula (37) can be reformulated as (see Appendix C for details):

$$f(\underline{x})=\sum_{p=1}^{P}\left[\sum_{l=1}^{L_p}\sum_{\underline{m}\in\mathbb{Z}^D}f(T_p\underline{m}+\underline{x}_p)\times e^{-j2\pi\widetilde{\underline{k}}_{p,l}^T\widetilde{M}_p^{-1}\underline{m}}h_{p,l}(\underline{x}-T_p\underline{m})\right] \quad (39)$$

where

$$\widehat{h}_{p,l}(\underline{\omega})=\frac{1}{|\det(M_p)|}\sum_{r=1}^{L_p}e^{j(\underline{\omega}-2\pi T^{-T}\widetilde{\underline{k}}_{p,l})^TT_p\widetilde{\underline{m}}_{p,r}}\widehat{\varphi}_{p,r}(\underline{\omega}). \quad (40)$$

In (39), for every p in the square brackets, we have exactly the configuration described in Fig. 3. Indeed, as stated earlier, (39) is the motivation for the general configuration we considered in our Interpolation Identity.

Next, we consider the case of discrete filtering. Using the Interpolation Identity of Theorem 1, the reconstruction can be carried out as depicted in Fig. 9, where R_p and M_p are as in (29), and the filters $\widehat{\tilde{h}}_p$ are given by [see (11)]

$$\widehat{\tilde{h}}_p(\underline{\omega})=\frac{L_p}{|\det(T_Q)|}\sum_{\underline{n}\in\mathbb{Z}^D}\sum_{l=1}^{L_p}\widehat{h}_{p,l}\times\left(\underline{\omega}-2\pi T_Q^{-T}\underline{k}_{p,l}+2\pi T_Q^{-T}M_p^T\underline{n}\right) \quad (41)$$

where $\{\underline{k}_{p,l}\}_{l=1}^{L_p}=\mathcal{SR}(M_p^T)$. This leads to samples on a Nyquist lattice. Finally, the original signal can be reconstructed via a simple lowpass filter, as shown on the far right-hand side of Fig. 9.

VI. Conclusion

This paper has presented a generalized interpolation identity applicable to multidimensional signals. The identity establishes the equivalence of two multidimensional processing operations. The key point here is that one of these utilizes discrete processing operations and leads to the data being transferred to a "Nyquist lattice" from which the continuous signal, if required, can be readily reconstructed by a simple multidimensional lowpass filter. We have also illustrated the application of the result to the special case of recurrent sampling. Beyond the cases discussed, we anticipate that the multidimensional result presented here will find wide spread application, as already exemplified in [4] for the 1-D case. In fact, the authors have been using the result presented here in a variety of multivariable reconstruction problems.

Appendix A
Proof of Lemma 1

Proof: From the definitions of $\mathcal{SR}(M^T)$, $\mathcal{SR}(\widetilde{M}^T)$, and (9), we have that for every $\underline{k}\in\mathcal{SR}(M^T)$, there exists a $\widetilde{\underline{k}}\in\mathcal{SR}(\widetilde{M}^T)$ such that $\widetilde{\underline{k}}=\rho(\underline{k})$. Hence, the mapping is onto. We use contradiction to establish the one-to-one property. Assume the converse of the result, i.e., suppose that $\rho(\underline{k}_1)=\rho(\underline{k}_2)$ for some $\underline{k}_1\neq\underline{k}_2\in\mathcal{SR}(M^T)$. Then, by (9), for some $\underline{n}_1$, $\underline{n}_2\in\mathbb{Z}^D$, we have

$$\widetilde{R}^T\underline{k}_1-\widetilde{M}^T\underline{n}_1=\widetilde{R}^T\underline{k}_2-\widetilde{M}^T\underline{n}_2$$

or

$$\widetilde{R}^T(\underline{k}_1-\underline{k}_2)=\widetilde{M}^T(\underline{n}_1-\underline{n}_2)=\underline{\ell}\in\mathbb{Z}^D. \quad (42)$$

Hence, $\underline{\ell}\in\{\widetilde{R}^T\underline{k}:\underline{k}\in\mathbb{Z}^D\}\cap\{\widetilde{M}^T\underline{n}:\underline{n}\in\mathbb{Z}^D\}$. However, using (3), we observe that

$$\{\widetilde{R}^T\underline{k}:\underline{k}\in\mathbb{Z}^D\}\cap\{\widetilde{M}^T\underline{n}:\underline{n}\in\mathbb{Z}^D\}=\{\widetilde{R}^TM^T\underline{m}:\underline{m}\in\mathbb{Z}^D\}=\{\widetilde{M}^TR^T\underline{m}:\underline{m}\in\mathbb{Z}^D\}.$$

Thus, for some $\underline{m}\in\mathbb{Z}^D$, (42) implies that

$$\underline{\ell}=\widetilde{R}^T(\underline{k}_1-\underline{k}_2)=\widetilde{R}^TM^T\underline{m}$$

namely

$$\underline{k}_1-\underline{k}_2=M^T\underline{m}\Leftrightarrow\underline{k}_1\equiv\underline{k}_2\bmod(M^T).$$

However, since $\underline{k}_1$, $\underline{k}_2\in\mathcal{SR}(M^T)\subset\mathcal{UC}(M^T)$, this necessarily implies that $\underline{k}_1=\underline{k}_2$. This leads to a contradiction. Thus, the claim is true. ■

APPENDIX B
PROOF OF THEOREM 1

Proof: To establish the identity, we will derive expressions for the outputs of the configurations in Figs. 3 and 4. We show that for the same input, they are equal if (11) is satisfied. In Fig. 3, we denote the input to the ℓth filter by $s_\ell(\underline{x})$. Then

$$\begin{aligned} s_\ell(\underline{x}) &= f_c(\underline{x}) \sum_{\underline{n}\in\mathbb{Z}^D} e^{-j2\pi \widetilde{\underline{k}}_\ell^T \widetilde{M}^{-1}\underline{n}} \delta(\underline{x}-T\underline{n}) \\ &= f_c(\underline{x}) e^{-j2\pi \widetilde{\underline{k}}_\ell^T \widetilde{M}^{-1}T^{-1}\underline{x}} \sum_{\underline{n}\in\mathbb{Z}^D} \delta(\underline{x}-T\underline{n}) \\ &\quad \ell = 1,\ldots,N. \end{aligned} \tag{43}$$

The Fourier transform (FT) of $s_\ell(\underline{x})$ is

$$\widehat{s}_\ell(\underline{\omega}) = \frac{1}{|\det(T)|} \sum_{\underline{n}\in\mathbb{Z}^D} \widehat{f}_c(\underline{\omega} + 2\pi T^{-T}\widetilde{M}^{-T}\widetilde{\underline{k}}_\ell - 2\pi T^{-T}\underline{n})$$

and hence

$$\begin{aligned} \widehat{y}_c = \frac{1}{|\det(T)|} \sum_{\ell=1}^{N} \widehat{h}_\ell(\underline{\omega}) \\ \times \sum_{\underline{n}\in\mathbb{Z}^D} \widehat{f}_c(\underline{\omega} + 2\pi T^{-T}\widetilde{M}^{-T}\widetilde{\underline{k}}_\ell - 2\pi T^{-T}\underline{n}). \end{aligned} \tag{44}$$

We next turn to the configuration in Fig. 4. The Fourier transform of $f(\underline{x}) = f_c(\underline{x})\sum_{\underline{n}\in\mathbb{Z}^D}\delta(\underline{x}-T\underline{n})$ is

$$\widehat{f}(\underline{\omega}) = \frac{1}{|\det(T)|} \sum_{\underline{n}\in\mathbb{Z}^D} \widehat{f}_c(\underline{\omega} - 2\pi T^{-T}\underline{n}).$$

Since we use continuous frequency, the expansion operation by R to generate $f_e(\underline{x})$ does not affect the spectrum. Hence

$$\begin{aligned} \widehat{f}_e(\underline{\omega}) &= \widehat{f}(\underline{\omega}) \\ &= \frac{1}{|\det(T)|} \sum_{\underline{n}\in\mathbb{Z}^D} \widehat{f}_c(\underline{\omega} - 2\pi T^{-T}\underline{n}). \end{aligned} \tag{45}$$

However, since the signals $f_e(\underline{x})$ and $y_e(\underline{x})$ are sampled on the lattice $\mathcal{LAT}(TR^{-1})$, the filter $\widetilde{h}(\underline{x})$ has the property that its frequency response satisfies the following periodicity property:

$$\widehat{\widetilde{h}}(\underline{\omega} + 2\pi T^{-T}R^T\underline{m}) = \widehat{\widetilde{h}}(\underline{\omega}) \text{ for all } \underline{m}\in\mathbb{Z}^D. \tag{46}$$

Furthermore, it can be shown that the multidimensional decimation effect via M can be described in the frequency domain by

$$\widehat{y}_d(\underline{\omega}) = \frac{1}{N}\sum_{\ell=1}^{N} \widehat{y}_e(\underline{\omega} + 2\pi T^{-T}R^T M^{-T}\underline{k}_\ell) \tag{47}$$

where we recall that $\underline{k}_\ell \in \mathcal{SR}(M^T) = \mathcal{UC}(M^T)\cap\mathbb{Z}^D$ and $N = |\det(M)| = |\det(\widetilde{M})|$. Now, since $\widehat{y}_e(\underline{\omega}) = \widehat{\widetilde{h}}(\underline{\omega})\widehat{f}_e(\underline{\omega})$, we have

$$\begin{aligned} \widehat{y}_d(\underline{\omega}) = \frac{1}{N}\sum_{\ell=1}^{N} \widehat{\widetilde{h}}(\underline{\omega} + 2\pi T^{-T}R^T M^{-T}\underline{k}_\ell) \\ \times \widehat{f}_e(\underline{\omega} + 2\pi T^{-T}R^T M^{-T}\underline{k}_\ell). \end{aligned}$$

Then

$$\begin{aligned} \widehat{y}_c(\underline{\omega}) &= \widehat{h}_{LP}(\underline{\omega})\widehat{y}_d(\underline{\omega}) \\ &= \frac{1}{N}\widehat{h}_{LP}(\underline{\omega}) \sum_{\ell=1}^{N} \widehat{\widetilde{h}}(\underline{\omega} + 2\pi T^{-T}R^T M^{-T}\underline{k}_\ell) \\ &\quad \times \widehat{f}_e(\underline{\omega} + 2\pi T^{-T}R^T M^{-T}\underline{k}_\ell). \end{aligned}$$

Substituting into (45), we obtain

$$\begin{aligned} \widehat{y}_c(\underline{\omega}) = \frac{1}{N|\det(T)|}\widehat{h}_{LP}(\underline{\omega}) \sum_{\ell=1}^{N} \widehat{\widetilde{h}}(\underline{\omega} + 2\pi T^{-T}R^T M^{-T}\underline{k}_\ell) \\ \times \sum_{\underline{n}\in\mathbb{Z}^D} \widehat{f}_c(\underline{\omega} + 2\pi T^{-T}R^T M^{-T}\underline{k}_\ell - 2\pi T^{-T}\underline{n}). \end{aligned}$$

Using (3) and Lemma 1, the above expression can be rewritten as

$$\begin{aligned} \widehat{y}_c(\underline{\omega}) = \frac{1}{N|\det(T)|}\widehat{h}_{LP}(\underline{\omega}) \sum_{\ell=1}^{N} \widehat{\widetilde{h}}(\underline{\omega} + 2\pi T^{-T}R^T M^{-T}\underline{k}_\ell) \\ \times \sum_{\underline{n}\in\mathbb{Z}^D} \widehat{f}_c(\underline{\omega} + 2\pi T^{-T}\widetilde{M}^{-T}\widetilde{R}^T\underline{k}_\ell - 2\pi T^{-T}\underline{n}). \end{aligned}$$

Applying Lemma 1 and (9) and (10), we obtain

$$\begin{aligned} &\widehat{y}_c(\underline{\omega}) \\ &= \frac{1}{N|\det(T)|}\widehat{h}_{LP}(\underline{\omega}) \sum_{\ell=1}^{N} \widehat{\widetilde{h}}(\underline{\omega} + 2\pi T^{-T}R^T M^{-T}\underline{k}_\ell) \\ &\times \sum_{\underline{n}\in\mathbb{Z}^D} \widehat{f}_c\left(\underline{\omega} + 2\pi T^{-T}\widetilde{M}^{-T}(\widetilde{M}^T\underline{n}_\ell + \widetilde{\underline{k}}_\ell) - 2\pi T^{-T}\underline{n}\right) \\ &= \frac{1}{N|\det(T)|}\widehat{h}_{LP}(\underline{\omega}) \sum_{\ell=1}^{N} \widehat{\widetilde{h}}(\underline{\omega} + 2\pi T^{-T}R^T M^{-T}\underline{k}_\ell) \\ &\times \sum_{\underline{n}\in\mathbb{Z}^D} \widehat{f}_c(\underline{\omega} + 2\pi T^{-T}\widetilde{M}^{-T}\widetilde{\underline{k}}_\ell - 2\pi T^{-T}\underline{n}). \end{aligned} \tag{48}$$

Comparing (44) to (48), we observe that the two outputs are equal if

$$\widehat{h}_\ell(\underline{\omega}) = \frac{1}{N}\widehat{h}_{LP}(\underline{\omega})\widehat{\widetilde{h}}(\underline{\omega} + 2\pi T^{-T}R^T M^{-T}\underline{k}_\ell)$$
$$\text{for every } \underline{\omega}\in\mathcal{UC}\left(2\pi T_Q^{-T}\right) \text{ and } \ell = 1,2,\ldots,N$$

or

$$\widehat{h}_\ell(\underline{\omega}) = \frac{1}{N}\widehat{h}_{LP}(\underline{\omega})\widehat{\widetilde{h}}\left(\underline{\omega} + 2\pi T_Q^{-T}\underline{k}_\ell\right)$$
$$\text{for every } \underline{\omega}\in\mathcal{UC}\left(2\pi T_Q^{-T}\right) \text{ and } \ell = 1,2,\ldots,N.$$

Equation (11) follows. This completes the proof of the theorem. ■

APPENDIX C
DERIVATION OF (39)

We begin by restating the reconstruction formula (38):

$$f(\underline{x}) = \sum_{p=1}^{P}\sum_{r=1}^{L_p}\sum_{\underline{n}\in\mathbb{Z}^D} f(T\underline{n} + \underline{x}_p + T_p\widetilde{\underline{m}}_{p,r})\varphi_{p,r}(\underline{x} - T\underline{n})$$

which can also be rewritten as

$$f(\underline{x})=\sum_{p=1}^{P}\sum_{r=1}^{L_p}\left[f(\underline{x}+\underline{x}_p+T_p\widetilde{\underline{m}}_{p,r})\sum_{\underline{n}\in\mathbb{Z}^D}\delta(\underline{x}-T\underline{n})\right]*\varphi_{p,r}(\underline{x}).$$

Then, in the frequency domain, we obtain

$$\widehat{f}(\underline{\omega})=\frac{(2\pi)^D}{|\det(T)|}\sum_{\underline{n}\in\mathbb{Z}^D}\widehat{f}(\underline{\omega}-2\pi T^{-T}\underline{n})\times\sum_{p=1}^{P}\sum_{r=1}^{L_p}e^{j(\underline{\omega}-2\pi T^{-T}\underline{n})^T(\underline{x}_p+T_p\widetilde{\underline{m}}_{p,r})}\widehat{\varphi}_{p,r}(\underline{\omega}). \quad (49)$$

Let $\{\widetilde{\underline{k}}_{p,l}\}_{l=1}^{L_p}=\mathcal{SR}(\widetilde{M}_p^T)$ so that, for every $\underline{n}\in\mathbb{Z}^D$, we can write $\underline{n}=\widetilde{M}_p^T\underline{m}+\widetilde{\underline{k}}_{p,l}$. Then, (49) can be rewritten as

$$\begin{aligned}\widehat{f}(\underline{\omega})&=\frac{(2\pi)^D}{|\det(T)|}\sum_{p=1}^{P}\sum_{\underline{m}\in\mathbb{Z}^D}\sum_{l=1}^{L_p}\widehat{f}\left(\underline{\omega}-2\pi T^{-T}\widetilde{\underline{k}}_{p,l}-2\pi T_p^{-T}\underline{m}\right)\\&\quad\times\sum_{r=1}^{L_p}e^{j\left(\underline{\omega}-2\pi T^{-T}\widetilde{\underline{k}}_{p,l}-2\pi T_p^{-T}\underline{m}\right)^T\underline{x}_p}\\&\quad\times e^{j(\underline{\omega}-2\pi T^{-T}\widetilde{\underline{k}}_{p,l})^TT_p\widetilde{\underline{m}}_{p,r}}\widehat{\varphi}_{p,r}(\underline{\omega})\end{aligned}$$

or

$$\begin{aligned}\widehat{f}(\underline{\omega})&=\sum_{p=1}^{P}\sum_{l=1}^{L_p}\left(\left[\widehat{f}(\underline{\omega}-2\pi T^{-T}\widetilde{\underline{k}}_{p,l})e^{j(\underline{\omega}-2\pi T^{-T}\widetilde{\underline{k}}_{p,l})^T\underline{x}_p}\right]\right.\\&\qquad\left.*\frac{(2\pi)^D}{|\det(T_p)|}\sum_{\underline{m}\in\mathbb{Z}^D}\delta\left(\underline{\omega}-2\pi T_p^{-T}\underline{m}\right)\right)\\&\quad\times\frac{1}{|\det(M_p)|}\sum_{r=1}^{L_p}e^{j(\underline{\omega}-2\pi T^{-T}\widetilde{\underline{k}}_{p,l})^TT_p\widetilde{\underline{m}}_{p,r}}\widehat{\varphi}_{p,r}(\underline{\omega}). \quad (50)\end{aligned}$$

Denoting

$$\widehat{h}_{p,l}(\underline{\omega})=\frac{1}{|\det(M_p)|}\sum_{r=1}^{L_p}e^{j(\underline{\omega}-2\pi T^{-T}\widetilde{\underline{k}}_{p,l})^TT_p\widetilde{\underline{m}}_{p,r}}\widehat{\varphi}_{p,r}(\underline{\omega})$$

and applying the inverse Fourier transform to (50), we obtain

$$\begin{aligned}f(\underline{x})&=\sum_{p=1}^{P}\sum_{l=1}^{L_p}\sum_{\underline{m}\in\mathbb{Z}^D}\left[f(T_p\underline{m}+\underline{x}_p)e^{-j(2\pi T^{-T}\widetilde{\underline{k}}_{p,l})^TT_p\underline{m}}\right.\\&\qquad\left.\times\delta(\underline{x}-T_p\underline{m})\right]*h_{p,l}(\underline{x})\\&=\sum_{p=1}^{P}\sum_{l=1}^{L_p}\sum_{\underline{m}\in\mathbb{Z}^D}\left[f(T_p\underline{m}+\underline{x}_p)e^{-j2\pi\widetilde{\underline{k}}_{p,l}^T\widetilde{M}_p^{-1}\underline{m}}\right.\\&\qquad\left.\times\delta(\underline{x}-T_p\underline{m})\right]*h_{p,l}(\underline{x})\end{aligned}$$

where we have used (31). The result (39) then follows.

REFERENCES

[1] K. F. Cheung, "A multidimensional extension of Papoulis' generalized sampling expansion with application in minimum density sampling," in *Advanced Topics in Shannon Sampling and Interpolation Theory*, R. J. Marks II, Ed. New York: Springer-Verlag, 1993, pp. 86–119.

[2] E. Dubois, "Motion-compensated filtering of time-varying images," *Multidimensional Syst. Signal Process.*, vol. 3, pp. 211–239, 1992.

[3] R. J. Marks II, Ed., *Advanced Topics in Shannon Sampling and Interpolation Theory*. New York: Springer-Verlag, 1993.

[4] Y. C. Eldar and A. V. Oppenheim, "Filterbank reconstruction of bandlimited signals from nonuniform and generalized samples," *IEEE Trans Signal Process.*, vol. 48, no. 10, pp. 2864–2875, Oct. 2000.

[5] B. L. Evans, "Designing commutative cascades of multidimensional upsamplers and downsamplers," *IEEE Signal Process. Lett.*, vol. 4, no. 11, pp. 313–316, Nov. 1997.

[6] A. Feuer, "On the necessity of Papoulis result for multidimensional (GSE)," *IEEE Signal Process. Lett.*, vol. 11, no. 4, pp. 420–422, Apr. 2004.

[7] A. Feuer and G. C. Goodwin, *Sampling in Digital Signal Processing and Control*. Boston, MA: Birhauser, 1996.

[8] R. A. Gopinath and C. S. Burrus, "On upsampling, downsampling, and rational sampling rate filter banks," *IEEE Trans. Signal Process.*, vol. 42, no. 4, pp. 812–824, Apr. 1994.

[9] A. K. Jain, *Fundamentals of Digital Image Processing*. Englewood Cliffs, NJ: Prentice-Hall, 1989.

[10] J. Kovacevic and M. Vetterli, "The commutativity of up/downsampling in two dimensions," *IEEE Trans. Inf. Theory*, vol. 37, no. 3, pp. 695–698, May 1991.

[11] C. C. Macduffee, *Vectors and Matrices*. New York: Math. Assoc. Amer., 1953.

[12] M. Newman, *Integral Matrices*. New York: Academic, 1972.

[13] A. Papoulis, "Generalized sampling expansion," *IEEE Trans. Circuits Syst.*, vol. CAS-24, no. 11, pp. 652–654, Nov. 1977.

[14] W. K. Pratt, *Digital Image Processing*, 3rd ed: John Wiley & Sons, 2001.

[15] P. P. Vaidyanathan, *Multirate Systems and Filter Banks*. Englewood Cliffs, NJ: Prentice-Hall, 1993.

Arie Feuer (F'04) received the B.Sc. and M.Sc. degrees in mechanical engineering from the Technion–Israel Institute of Technology, Haifa, Israel (in 1967 and 1973, respectively) and the Ph.D. degree from Yale University, New Haven, CT, on 1978.

From 1967 to 1970, he was with Technomatics Inc., working on the design of automatic machines. From 1978 through 1983, he worked for Bell Labs in network performance evaluation. In 1983, joined the faculty of Electrical Engineering at the Technion, where he is currently a professor and head of the Control and Robotics Lab. Current research interests include resolution enhancement of digital images and videos, sampling and combined representations of signals and images, and adaptive systems in signal processing and control.

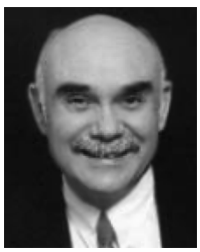

Graham C. Goodwin (F'86) received the B.Sc. degrees in physics, the B.E. degree in electrical engineering, and the Ph.D. degree from the University of New South Wales, Sydney, Audstralia.

From 1970 until 1974, he was a lecturer with the Department of Computing and Control, Imperial College, London, U.K. Since 1974, he has been with the Department of Electrical and Computer Engineering, The University of Newcastle, Callaghan, Australia. He is the co-author of eight monographs, four edited volumes, and several hundred technical papers. He is currently Professor of electrical engineering and Associate Director of the Centre for Complex Dynamic Systems and Control, the University of Newcastle, and a Director of National ICT, Australia.

Dr. Goodwin has received several international prizes, including the USA Control Systems Society 1999 Hendrik Bode Lecture Prize, a Best Paper award by IEEE TRANSACTIONS ON AUTOMATIC CONTROL, a Best Paper award by Asian Journal of Control, and a Best Engineering Text Book award from the International Federation of Automatic Control. He is the recipient of an ARC Federation Fellowship; an Honorary Fellow of Institute of Engineers, Australia; a Fellow of the Australian Academy of Science; a Fellow of the Australian Academy of Technology, Science, and Engineering; a Member of the International Statistical Institute; a Fellow of the Royal Society, London; and a Foreign Member of the Royal Swedish Academy of Sciences.